

RUSSIAN ACADEMY OF SCIENCE
Lenin Order of Siberian Branch
G.I. BUDKER INSTITUTE OF NUCLEAR PHYSICS

D.V. Pestrikov

DIPOLE BEAM BREAKUP
ELECTRON CLOUD INSTABILITY
OF A RELATIVISTIC POSITRON BUNCH
WITH A SMOOTH MODEL
LINEAR DENSITY

Budker INP 2005-6

Novosibirsk
2005

**Dipole beam breakup electron cloud instability
of a relativistic positron bunch
with a smooth model linear density**

D. V. Pestrikov

Budker Institute of Nuclear Physics
630090, Novosibirsk, Russia

Abstract

We study the beam breakup instability of the dipole coherent oscillations of the relativistic positron bunch interacting with initially unperturbed electron cloud. We assume a special distribution of the linear density of positrons along the bunch which enables the calculations of analytic solutions of the linearized equations of motion of the cloud electrons. With these assumptions equations describing centroid beam breakup oscillations of the cloud and of the bunch can be solved taking into account effects of the cloud pinching and associated BNS damping. Although the BNS damping does not eliminate the electron cloud instability of coherent oscillations of the bunch, it changes the dependencies of the coherent oscillation amplitudes on the time from the quasi-exponential to the power function ones.

1 Introduction

Positron, or proton beams can produce in the vacuum chambers of storage rings big amounts of secondary low energy electrons. The space charge fields of the beam focus these electrons towards the closed orbit of the beam. Typical filling patterns of the beam by its bunches do not provide stability conditions for oscillations of these electrons relative the beam closed orbit. As a result, secondary electrons leave the beam after being passed by several beam bunches. However, if the electron production rate is large enough, this phenomenon can result in collections near the closed orbit of electron clouds. One or, more gaps in the filling pattern of the beam usually serve to clean the orbit from these clouds. So that to the next turn the beam particles produce a fresh cloud. The space charge fields of these clouds perturb the oscillations of the beam particles resulting in the electron cloud instability. This manifold phenomenon can manifest itself through the instabilities of either incoherent or coherent oscillations of the beam. In particular, the authors of Ref.[1] have suggested to explain the observed blowups of transverse positron bunch sizes in electron-positron factories KEKB and PEP-II (see, e.g. in Refs.[2] and [3]) as a result of some head-tail singlebunch dipole instability due to interactions of the beam bunches with the electron clouds. Till now several candidates are considered as a driving head-tail instability to explain particular effects. Although weak solenoidal magnetic fields increase the threshold currents of electron cloud instability [4], it still does not allow, for instance, the high-current operations of KEKB with small distances between the neighbor bunches in the positron beam.

General descriptions of coupled oscillations of a single bunch in the beam and of the cloud encounters heavy mathematical difficulties. Very frequently these calculations are simplified employing the rigid bunch model where coherent oscillations of the bunch and of the cloud are described as the oscillations of their centroids (for example, in Refs.[1] and [5]). However, even in this approximation the resulting equations describing the coupling of even dipole coherent oscillations of the bunch and of the cloud still are very complicated for their direct analytic solutions. We can point out at least two important features embarrassing such calculations.

First, in most realistic cases the linear density of the bunch is a smooth function of the longitudinal distance in the bunch (z). Usually, it means that the frequencies of the oscillations of the cloud electrons (Ω_c) vary during the bunch passage. As a result, the equations describing the motions of electrons enable their analytic solutions only in special cases. The simplest case, when the bunch linear density is a rectangular function of z was studied in many details in e.g. Refs.[1] and [6]. In this model, the frequencies Ω_c are constant. So that the frequency spreads of the cloud electrons can appear only due to nonlinear dependencies of the bunch space charge fields on transverse coordinates. The frequencies Ω_c of the cloud electrons interacting with the bunch having a smooth linear density vary between zero and the maximum value corresponding to that of the linear density. In this case, the values Ω_c are distributed within relevant frequency interval even for linear dependencies of the bunch space charge forces on the transverse electron positions. An example of the calculations taking into account smooth variations of the bunch linear density was given in Ref.[5]. However, due to several incorrectness in the calculations and assumptions (see, e.g. in Ref.[7]) this paper gives wrong predictions for both initial and asymptotic behavior of the amplitudes of coherent oscillations of the bunch.

Second, during the bunch passage the electron cloud tends to be pinched near the closed orbit. Generally, this pinching increases the space charge fields of the electron cloud and results in the variations of the betatron tune shifts of the bunch particles along the bunch. If the cloud pinching is strong, that can result in the BNS damping (see, e.g. in Ref.[8]) of coherent oscillations of the bunch and affect the asymptotic behavior of the amplitudes of these oscillations.

In this paper we study stability of the linear dipole betatron oscillations of a positron bunch in the electron cloud within the framework of the rigid bunch model and assuming the beam breakup regime. For this reason, we neglect in our calculations the longitudinal mobility of particles (positrons and electrons). We also assume that at a given position s on the closed orbit of positrons the unperturbed electron cloud is prepared by preceding bunches of the beam. Coherent oscillations of the bunch are described by the local centroids which depend both on the time and on the distance along the bunch. We assume that the oscillations of the electron cloud are excited by the oscillations of the bunch uniformly along the closed orbit. We shall use a special smooth model expression for the linear density of the bunch which enables exact solutions to the linearized equations of motion of the cloud electrons.

Although such an approach gives a limiting view on the problem, it en-

ables one to simplify the required calculations and to study the specific features of the development of dipole singlebunch oscillations in many details. For the bunches in a storage ring the beam breakup approximation may hold well, if the frequency shifts of the coherent oscillations substantially exceed the frequency of the synchrotron oscillations of particles. This approach gives also adequate description of coherent fluctuations of the bunch in the case, when these fluctuations are generated with the average frequency substantially exceeding the frequency of the synchrotron oscillations of the particles.

We shall ignore the interactions of bunches in the beam. Partially, this is based on the expectation that the main contribution to the singlebunch interaction give the electrons in the close vicinity of the bunch. Due to strong overfocusing of these electrons by the space charge fields of the bunch to the time when the next bunch arrives at the perturbed cloud the most of such electrons are removed to deep peripheral regions of the bunch, or out of the vacuum chamber of the ring. For this reason and in agreement with observations in e.g. positron storage ring of KEKB, we may expect that the multibunch instabilities are depressed as compared to the singlebunch ones.

We simplify our calculations assuming that the cloud electrons are not affected by external fields during the bunch passage. For example, that may occur in straight sections of the ring. In the straight sections containing the solenoidal fields (say, of the strength B) these calculations will give correct results provided that the bunch length (σ_s) is small:

$$\chi = \frac{eB\sigma_s}{mc^2} \ll 1. \quad (1)$$

Here, e is the charge of the electron, m is its mass and c is the speed of light. The condition in Eq.(1) holds well for typical parameters of B-factories except maybe the interaction point. For example, if we take $B = 50$ G and $\sigma_s = 5$ mm, we obtain $\chi \simeq 0.015$. However, for a bunch which is 100 times longer (e.g. $\sigma_s = 50$ cm) the parameter χ increase up to $\chi \simeq 1.5$. In the last case, the cloud centroid equations should take into account the perturbations of electrons by the magnetic fields of the solenoids.

2 Oscillations of the cloud centroids

We study the linear coherent oscillations of the cloud and of the bunch. Correspondingly, the forces in all equations of motion will be calculated in the linear approximation in the centroid coordinates. The motions of particles are described using x as the horizontal coordinate of a particle, y – as the

vertical coordinate and z as the longitudinal distance in the bunch from its synchronous particle. We define as $s = vt + z$ the length of the closed orbit passed by the bunch particle to the time t . Assuming the studying of the singlebunch oscillations we neglect the longitudinal motion of electrons. We define as σ_x and σ_y the rms transverse horizontal and vertical bunch sizes ($\sigma_x > \sigma_y$) and as b the radius of the cross section of the vacuum chamber. Then, omitting the values of the order of $(\sigma_x/b) \ll 1$, we neglect the fields of the charge images in the walls of the vacuum chamber. We describe the dipole coherent oscillations of the bunch and of the cloud using the coordinates of their centers of the gravity (the coordinates of their centroids). For vertical coherent oscillations at the point s of the orbit we write $y_c = y_c(t, s)$ for the cloud centroid. Since the bunch moves along the closed orbit with the average velocity v , we write $y_b = y_b(s - vt, s)$.

At least for B-factory parameters, the typical value of the electron cloud density on the closed orbit of the bunch is substantially lower than that of the bunch. For this reason, if we study the singlebunch coherent oscillations, the effects of the space charge fields of the cloud on electron motions can be neglected. Assuming that the bunch particles are relativistic ones so that their Lorentz factors $\gamma = 1/\sqrt{1 - (v/c)^2}$ are large, we find that the force acting on electrons at the position s on the closed orbit is proportional to the bunch linear density $\lambda_b(s - vt)$ and depends on the transverse coordinates of electrons in the combinations x and $y - y_b(s - vt, s)$. Averaging equations of motion for individual electrons, we obtain the equations describing the evolution of the cloud centroids. For the linear vertical oscillations this equation reads

$$\frac{d^2 y_c}{dt^2} = -\omega_c^2 g(z) [y_c(t, s) - y_b(z, s)], \quad g(z) = \frac{\lambda_b(z)}{\lambda_b(0)}. \quad (2)$$

The value of the frequency ω_c in this equation as well as its dependencies on transverse sizes of the bunch and of the cloud depends on the model which is used to obtain Eq.(2) (see, e.g. in Ref.[9]). Generally, the force acting on electrons is a nonlinear function of the electron coordinates. The result of the averaging depends on the consequence of the averaging and of the linearization of the equation. If we average the linearized equations for electrons then, the frequency ω_c depends on the transverse sizes of the bunch only. For example, if the transverse distribution in the bunch is a Gaussian, we obtain

$$\omega_c^2 = \frac{2N_b e^2 \lambda_b(0)}{m\sigma_y(\sigma_x + \sigma_y)}. \quad (3)$$

On the contrary, if we average nonlinear equations of motion and then calcu-

late the linear part of the average force, we shall find that the parameter ω_c depends on the transverse sizes of the bunch and of the cloud. For example, if the transverse distributions in the bunch and in the cloud are Gaussian, the parameter ω_c reads

$$\omega_c^2 = \frac{2N_b e^2 \lambda_b(0)}{m \Sigma_y (\Sigma_x + \Sigma_y)}. \quad (4)$$

Here, $\Sigma_x^2 = \sigma_x^2 + \sigma_{xc}^2$ and $\Sigma_y^2 = \sigma_y^2 + \sigma_{yc}^2$, σ_{xc} and σ_{yc} are the rms horizontal and vertical cloud sizes. More complicated dependencies of ω_c on the transverse bunch and cloud sizes can be obtained for non-Gaussian density distributions in the cloud. For any transverse cloud density distribution we conclude that in this model the parameter ω_c will depend on the transverse cloud sizes only, if the cloud is wider than the bunch. In the last case, the parameter ω_c will depend on z provided that transverse cloud sizes vary during the bunch passage. In this paper we simplify calculations assuming that equations of motion of electrons are linearized before their averaging. Correspondingly, we define ω_c using Eq.(3).

Now, we note that at a given position on the closed orbit s the driving force in Eq.(2) depends on time only in the combination $z = s - vt$. Taking in Eq.(2) z as a new independent variable, we obtain

$$\frac{d^2 y_c(z, s)}{dz^2} + k_c^2 g(z) y_c(z, s) = k_c^2 g(z) y_b(z, s), \quad (5)$$

where $k_c = \omega_c/v$. Assuming that the width of the function $g(z)$ is determined by the bunch length σ_s and defining

$$x = \frac{z}{\sigma_s}, \quad q^2 = k_c^2 \sigma_s^2, \quad (6)$$

we rewrite Eq.(5) in the form:

$$y_c''(x, s) + q^2 g(x) y_c(x, s) = q^2 g(x) y_b(x, s), \quad (7)$$

where $y' = dy/dx$. In this paper we neglect all effects of multibunch interactions as well as noise excitations of coherent oscillations of the electron cloud. Then, Eq.(5) should be solved using zero initial conditions.

$$y_c(\infty, s) = 0, \quad y_c'(\infty, s) = 0. \quad (8)$$

Following the paper [5], we shall calculate solutions to Eq.(7) using two linearly independent solutions to the homogeneous part of Eq.(7):

$$y_{1,2}''(x, s) + q^2 g(x) y_{1,2}(x, s) = 0. \quad (9)$$

This equation shows that conditions for free coherent oscillations of electrons do not depend on s . Therefore, below we can write $y_{1,2}(x, s) = y_{1,2}(x)$. The functions $y_{1,2}$ will be normalized using any convenient value for their Wronskian:

$$W = y_1(x)y_2'(x) - y_1'(x)y_2(x). \quad (10)$$

For bunches with smooth linear densities the function $g(x)$ is defined in the interval $|x| \leq \infty$. Since W is an integral of motion ($dW/dx = 0$), one of the functions $y_{1,2}(x)$, or both of them can infinitely grow, when $|x| \rightarrow \infty$. Below, we shall also use the following limiting conditions for the functions $y_{1,2}$:

$$y_{10} = \lim_{x \rightarrow \infty} y_1(x) = 1, \quad \lim_{x \rightarrow \infty} \left[\frac{dy_1(x)}{dx} y_2(x) \right] = 0, \quad (11)$$

and

$$y_{20}' = \lim_{x \rightarrow \infty} \frac{dy_2(x)}{dx} = W. \quad (12)$$

Solutions to Eq.(7) read

$$y_c(x, s) = A(x)y_1(x) + B(x)y_2(x). \quad (13)$$

Substituting this expression in Eq.(7), using the condition $y' = A(x)y_1'(x) + B(x)y_2'(x)$ and initial conditions from Eq.(8), we find

$$y_c(x, s) = - \int_x^\infty dx_1 g(x_1) K(x, x_1) y_b(x_1, s), \quad (14)$$

where the kernel $K(x, x_1)$ reads

$$K(x, x_1) = \pi q^2 (y_1(x)y_2(x_1) - y_2(x)y_1(x_1)), \quad (15)$$

and we took $W = -1/\pi$. We note that $K(x, x) = 0$ and that for close longitudinal coordinates in the bunch ($x_1 = x + \delta x$, $\delta x \ll x$)

$$K(x, x_1) = -q^2(x_1 - x) + O[(x_1 - x)^3], \quad (16)$$

the kernel $K(x, x_1)$ linearly depends on $x_1 - x$. Outside this region the kernel $K(x, x_1)$ in Eq.(14) does not depend on the difference $x_1 - x$ unless the linear density ($g(x)$) is constant along the bunch (see e.g. in the Appendix 7).

3 Oscillations of the bunch centroids

Within the framework of the rigid bunch model and within the smoothed focusing approximation the dipole coherent oscillations of the relativistic bunch ($\gamma \gg 1$) are described using the following centroid equation:

$$\frac{d^2 y_b(x, s)}{ds^2} + k_\beta^2 y_b(x, s) = -k_b^2(x) [y_b(x, s) - y_c(x, s)]. \quad (17)$$

Here, $k_\beta = \nu_\beta/R_0$, ν_β is the frequency of betatron oscillations of the bunch particles in the storage ring, $\Pi = 2\pi R_0$ is the perimeter of the closed orbit and s is an independent variable. The coupling coefficient k_b should be calculated within the same approach as the parameter ω_c in Eq.(2). If equations of motion are linearized prior to their averaging and if we define as n_0 the density of the cloud at the closed orbit, the parameter k_b reads

$$k_b^2 = \frac{2\pi n_0 r_0}{\gamma}. \quad (18)$$

Here, $r_0 = e^2/mc^2$ is the classical radius of a bunch particle. For simplicity we assume that the conditions of the cloud electron productions are uniform along the closed orbit. It means that the unperturbed value of n_0 does not depend on s . During the bunch passage of a point s on the closed orbit the cloud density n_0 increases due to approaching to the closed orbit of electrons kicked by previous parts of the bunch (the cloud pinching). For this reason, the values n_0 and k_b^2 in Eq.(18) at the point s depend on x .

Substituting in Eq.(17) the value of $y_c(x, s)$ from Eq.(14), we obtain

$$\begin{aligned} \frac{d^2 y_b(x, s)}{ds^2} + k_\beta^2 y_b(x, s) = & -k_b^2(x) y_b(x, s) \\ & - k_b^2(x) \int_x^\infty dx_1 g(x_1) K(x, x_1) y_b(x_1, s). \end{aligned} \quad (19)$$

Now, we define

$$\zeta_1 = \frac{1}{k_\beta} \frac{dy_b}{ds} - iy_b, \quad \zeta_{-1} = \frac{1}{k_\beta} \frac{dy_b}{ds} + iy_b, \quad y_b = \frac{\zeta_{-1} - \zeta_1}{2i}. \quad (20)$$

In the smoothed focusing approximation the absolute value of the coordinates $\zeta_{\pm 1}$ gives the amplitude of the dipole oscillations of the bunch:

$$|\zeta_{\pm 1}|^2 = \left(\frac{1}{k_\beta} \frac{dy_b}{ds} \right)^2 + y_b^2. \quad (21)$$

According to Eq.(20) the value ζ_1 obeys the following equation:

$$\begin{aligned} \frac{d\zeta_1}{ds} = & -ik_\beta\zeta_1 - \frac{k_b^2}{k_\beta} \frac{[\zeta_{-1}(x, s) - \zeta_1(x, s)]}{2i} \\ & - \frac{k_b^2}{k_\beta} \int_x^\infty dx_1 g(x_1) K(x, x_1) \frac{\zeta_{-1}(x_1, s) - \zeta_1(x_1, s)}{2i}. \end{aligned} \quad (22)$$

Assuming that the interaction with the cloud results in the frequency shifts which are substantially smaller than the frequency of unperturbed betatron oscillations of particles ($k_b^2 \ll k_\beta^2$), we neglect in the right-hand side of Eq.(22) the contributions of the rapidly varying terms. This yields

$$\frac{d\zeta_1}{ds} = -i \left[k_\beta + \frac{k_b^2(x)}{2k_\beta} \right] \zeta_1(x, s) - i \frac{k_b^2(x)}{2k_\beta} \int_x^\infty dx_1 g(x_1) K(x, x_1) \zeta_1(x_1, s). \quad (23)$$

The second term in the square brackets gives the tuneshift of coherent oscillations of the bunch due to their perturbations by the cloud space charge fields

$$\Delta\nu_\beta = \frac{k_b^2(x)R_0}{2k_\beta} = \frac{n_0(x)r_0\beta_{av}\Pi}{2\gamma}, \quad (24)$$

where $\beta_{av} = R_0/\nu_\beta$ is the average value of the β -function of the ring. Using

$$\zeta_1(x, s) = e^{-ik_\beta s} X(x, s), \quad (25)$$

and defining as a new independent variable the value

$$u = \frac{(k_b^2)_{\max}}{2k_\beta} s, \quad (26)$$

where $(k_b^2)_{\max}$ is the value of the parameter k_b^2 corresponding e.g. to the maximum value of the cloud density at the point s during the bunch passage, we replace Eq.(26) by the following:

$$\frac{dX(x, u)}{du} = -ir(x)X(x, u) - ir(x) \int_x^\infty dx_1 g(x_1) K(x, x_1) X(x_1, u). \quad (27)$$

Here, $r(x) = k_b^2(x)/(k_b^2)_{\max}$. This equation can be solved using the Fourier transform in the variable u . Substituting in Eq.(27)

$$X(x, \omega) = \int_0^\infty du X(x, u) e^{i\omega u}, \quad (28)$$

$$X(x, u) = \int_{-\infty}^\infty \frac{d\omega}{2\pi} X(x, \omega) e^{-i\omega u}, \quad \text{Im}\omega > 0, \quad (29)$$

and integrating both sides in this equations with $e^{i\omega u}$ over u from zero to infinity, we obtain

$$X(x, \omega) = \frac{iX(x, 0)}{\omega - r(x)} + \frac{r(x)}{\omega - r(x)} \int_x^\infty dx_1 g(x_1) K(x, x_1) X(x_1, \omega). \quad (30)$$

Here, the function $X(x, 0)$ denotes the initial distribution of $X(x, u)$ along the bunch. Now, we define

$$X(x, \omega) = \frac{iX(x, 0)}{\omega - r(x)} + \frac{r(x)}{\omega - r(x)} P(x, \omega), \quad (31)$$

where

$$P(x, \omega) = \int_x^\infty dx_1 g(x_1) K(x, x_1) X(x_1, \omega). \quad (32)$$

Calculating the second derivative of P with respect to x and using Eq.(31), we find that P obeys the differential equation ¹:

$$\frac{d^2 P}{dx^2} + q^2 g(x) \frac{\omega}{\omega - r(x)} P(x, \omega) = \frac{-iq^2 g(x)}{\omega - r(x)} X(x, 0). \quad (33)$$

By its definition and since $\lim_{x \rightarrow \infty} g(x) = 0$, the function $P(x, \omega)$ obeys the border conditions:

$$P(\infty, \omega) = 0, \quad \left(\frac{dP}{dx} \right)_{x=\infty} = 0. \quad (34)$$

Similar to Eq.(7), we express the formal solution to Eq.(33) using the linearly independent solutions to the homogeneous part of this equation:

$$\frac{d^2 P_{1,2}}{dx^2} + q^2 g(x) \frac{\omega}{[\omega - r(x)]} P_{1,2}(x, \omega) = 0. \quad (35)$$

Assuming for $P_{1,2}(x)$ the limiting conditions similar to that in Eqs.(11) and (12):

$$P_{10} = \lim_{x \rightarrow \infty} y_1(x) = 1, \quad \lim_{x \rightarrow \infty} \left[\frac{dP_1(x)}{dx} P_2(x) \right] = 0,$$

$$P'_{20} = \lim_{x \rightarrow \infty} \frac{dP_2(x)}{dx} = W = -\frac{1}{\pi},$$

¹Equation (33) differs from relevant equations for the bunch centroid obtained in Ref.[5] (e.g. Eq.(A2)) for two reasons. First, according to Eqs.(14) and (17) in Ref.[5] the authors assume that the force perturbing the bunch centroids is proportional to the cloud centroid and vice versa. Contrary to our calculations, this assumption eliminates in Eq.(A2) of Ref.[5] the terms describing possible BNS-damping of the bunch oscillations. The second, wrong solution in Ref.[5] of Eqs.(38), or (41) cancels the right-hand side in Eq.(A2) of Ref.[5]. Corrections of these calculations result in Eq.(33) of this paper.

where

$$W = P_1 \frac{dP_2}{dx} - P_2 \frac{dP_1}{dx},$$

we find

$$\begin{aligned} P(x, \omega) &= -\frac{iq^2}{W} P_1(x) \int_x^\infty \frac{g(x_1)}{\omega - r(x_1)} X(x_1, 0) P_2(x_1) dx_1 \\ &+ \frac{iq^2}{W} P_2(x) \int_x^\infty \frac{g(x_1)}{\omega - r(x_1)} X(x_1, 0) P_1(x_1) dx_1. \end{aligned} \quad (36)$$

and

$$\begin{aligned} X(x, \omega) &= \frac{iX(x, 0)}{\omega - r(x)} + \frac{i\pi q^2 r(x) P_1(x, \omega)}{\omega - r(x)} \int_x^\infty \frac{g(x_1) X(x_1, 0) P_2(x_1, \omega)}{\omega - r(x_1)} dx_1 \\ &- \frac{i\pi q^2 r(x) P_2(x, \omega)}{\omega - r(x)} \int_x^\infty \frac{g(x_1) X(x_1, 0) P_1(x_1, \omega)}{\omega - r(x_1)} dx_1. \end{aligned} \quad (37)$$

If the functions $P_{1,2}(x, \omega)$ are known, this equation together with Eq.(29) enables the calculation of the bunch centroid accounting the cloud pinching and associated BNS damping of the electron cloud instability. The obtained expression for $X(x, \omega)$ is simplified for initial conditions where $X(x, 0) = X_0 \delta(x - x_0)$, or for the initial condition where $X(x, 0) = 1$. In the last case, simple calculations yield

$$X(x, \omega) = \frac{i}{\omega - r(x)} - \frac{ir(x)}{[\omega - r(x)]\omega} [1 - P_1(x, \omega)]. \quad (38)$$

So that the oscillation amplitude $X(x, \omega)$ is obtained using of the function $P_1(x, \omega)$ only.

4 No cloud pinching

The calculations on the electron cloud instability are simplified in the cases, when the cloud pinching can be neglected. Although this implies certain limitations on the region of the problem parameters, this approximation is frequently used in analytic calculations relating the electron cloud instability of coherent oscillations (see, e.g. in Ref.[6]). We shall obtain such solutions to compare the features of coherent oscillations of the bunch calculated taking into account the cloud pinching and calculated ignoring this effect.

If we neglect the variations of the transverse cloud sizes during the bunch passages, then we put in all relevant equations of the previous Section

$r(x) = 1$. Substituting this value in e.g. Eq.(35) and shifting in this equation ω by 1 ($\omega \rightarrow \omega + 1$), we obtain

$$\frac{d^2 P_{1,2}}{dx^2} + p^2 g(x) P_{1,2}(x, \omega) = 0, \quad p^2 = q^2 \left(1 + \frac{1}{\omega}\right). \quad (39)$$

This equation has the same form as Eq.(9). If we define the linearly independent solutions to Eq.(9) as $y_{1,2}(q, x)$, then the linearly independent solutions to Eq.(39) are obtained using

$$P_{1,2}(x, \omega) = y_{1,2}(p, x). \quad (40)$$

So that coherent oscillations of the cloud and of the bunch are determined using the same couple of the linearly independent functions $y_{1,2}(\kappa, x)$. For the cloud oscillations we substitute $\kappa^2 = q^2$, while for the bunch oscillations we should use $\kappa^2 = p^2$. Substituting Eq.(40) in Eq.(37), we obtain

$$\begin{aligned} X(x, \omega) = & \frac{iX(x, 0)}{\omega} + \frac{i\pi q^2}{\omega^2} y_1(p, x) \int_x^\infty g(x_1) X(x_1, 0) y_2(p, x_1) dx_1 \\ & - \frac{i\pi q^2}{\omega^2} y_2(p, x) \int_x^\infty g(x_1) X(x_1, 0) y_1(p, x_1) dx_1. \end{aligned} \quad (41)$$

Provided that the functions $y_{1,2}(q, x)$ are known, Eq.(41) yields an exact expression for the Fourier-amplitudes of the centroid of the positron bunch interacting with electron cloud without pinching. The right-hand side in Eq.(41) can be simplified for several special initial distributions $X(x, 0)$.

1. If we take

$$X(x, 0) = X_0 \delta(x - x_0), \quad (42)$$

where $\delta(x)$ is the Dirac δ -function, then Eq.(41) results in

$$X(x, \omega) = \frac{iX_0 \delta(x - x_0)}{\omega} + \delta X(x, \omega), \quad (43)$$

where

$$\begin{aligned} \delta X(x, \omega) = & 0, \quad x > x_0 \\ \delta X(x, \omega) = & \frac{i\pi q^2}{\omega^2} X_0 g(x_0) [y_1(p, x) y_2(p, x_0) - y_2(p, x) y_1(p, x_0)], \quad x \leq x_0 \end{aligned} \quad (44)$$

According to this expression the amplitudes of the excited oscillations are smaller, if initial displacement (or, initial kick) in the bunch is shifted towards to its head.

2. If we take $X(x, 0) = 1$, then using Eq.(54) we obtain

$$X(x, \omega) = \frac{i}{\omega + 1} + \frac{i y_1(p, x)}{\omega(\omega + 1)}. \quad (45)$$

In this case, we can calculate $X(x, u)$, if we know the function $y_1(q, x)$ only.

3. Since

$$p^2 \int_x^\infty g(x_1) X(x_1, 0) y_2(p, x_1) dx_1 = X(x, 0) \frac{dy_2(p, x)}{dx} - X(\infty, 0) y'_{20} \quad (46)$$

$$+ \lim_{x \rightarrow \infty} \left[\frac{dX(x, 0)}{dx} y_2(p, x) \right] - \frac{dX(x, 0)}{dx} y_2(x) - \int_x^\infty \frac{d^2 X(x_1, 0)}{dx_1^2} y_2(p, x_1) dx_1,$$

a special case may present the initial conditions where

$$\frac{d^2 X(x, 0)}{dx^2} = -q^2 g(x) X(x, 0), \quad (47)$$

or $X(x, 0) = A y_1(q, x)$. For finite values of $X(\infty, 0)$ the function $y_2(q, x)$ may not contribute to $X(x, 0)$. Substituting this initial condition in Eq.(46) and then, in Eq.(41), using the conditions in Eqs.(11), (12), after simple calculations we obtain

$$X(x, \omega) = \frac{A y_1(p, x)}{-i\omega}. \quad (48)$$

The inverse Fourier transform yields the value $X(x, u)$:

$$X(x, u) = e^{-iu} \int_{-\infty}^\infty \frac{d\omega}{2\pi} X(x, \omega) e^{-i\omega u}, \quad \text{Im}\omega > 0. \quad (49)$$

All these expressions are useful only in the cases, when the functions can be calculated analytically. Apart from special distributions of the linear density along the bunch, that can be done calculating the asymptotic behavior of $X(x, u)$ at large times. For simplicity we take the initial condition in the form $X(x, 0) = y_1(q, x)$. Substituting Eq.(48) in Eq.(49), we find ($Z(x, u) = e^{iu} X(x, u)$)

$$Z(x, u) = \int_{-\infty}^\infty \frac{d\omega}{-2\pi i \omega} y_1 \left(q \sqrt{1 + \frac{1}{\omega}}, x \right) e^{-i\omega u}.$$

Changing here the integration variable $w = \omega u$, we rewrite this formula in the following form

$$Z(x, u) = \int_{-\infty}^\infty \frac{dw}{-2\pi i w} y_1 \left(q \sqrt{1 + \frac{u}{w}}, x \right) e^{-iw}. \quad (50)$$

According to Eq.(39) the function $y_1(p, x)$ in the integrand obeys the equation

$$\frac{d^2 y}{dx^2} + Q^2(x)y = 0, \quad Q^2 = q^2 \left(1 + \frac{u}{w}\right) g(x). \quad (51)$$

In the asymptotic region ($u \gg |w|$; we shall define the asymptotic region more precisely a bit later) we write

$$Q^2 \simeq \frac{q^2 u}{w} g(x). \quad (52)$$

Then, the linearly independent solutions to Eq.(51) can be found using the WKB method (e.g. in Ref.[10]). Simple calculations result in

$$y_1(p, x) \simeq \frac{(w/u)^{1/4}}{\sqrt{\pi q_1}} \cos \left(q_1 \sqrt{\frac{u}{w}} - \frac{\pi}{4} \right), \quad u \gg |w|. \quad (53)$$

and

$$y_2(p, x) \simeq \frac{(w/u)^{1/4}}{\sqrt{\pi q_1}} \sin \left(q_1 \sqrt{\frac{u}{w}} - \frac{\pi}{4} \right), \quad u \gg |w|. \quad (54)$$

where we defined

$$q_1 = q \int_x^\infty \sqrt{g(x_1)} dx_1. \quad (55)$$

Substituting Eq.(53) in Eq.(50), we obtain

$$Z(x, u) \simeq \frac{1}{-i(2\pi)^{3/2} u^{1/4} \sqrt{2q_1}} \int_{-\infty}^\infty \frac{dw}{w^{3/4}} \left[e^{-i\Phi_+(w)} + e^{-i\Phi_-(w)} \right], \quad (56)$$

where

$$\Phi_+(w) = w + q_1 \sqrt{\frac{u}{w}} - \frac{\pi}{4}, \quad \Phi_-(w) = w - q_1 \sqrt{\frac{u}{w}} + \frac{\pi}{4}. \quad (57)$$

The integration contour in Eq.(56) should not enter the regions where $q_1^2 u \ll |w|$. In the asymptotic region the main contribution to the integral in the right-hand side of Eq.(56) gives the vicinity of the saddle point ($d\Phi_\pm/dw = 0$)

$$w_1 = w_0 \frac{-1 + i\sqrt{3}}{2}, \quad w_0 = \left(\frac{q_1^2 u}{4} \right)^{1/3} \gg 1 \quad (58)$$

Calculating Gaussian integrals, we obtain

$$Z(x, u) \simeq \frac{i}{2\pi\sqrt{3}} \left(\frac{4}{q_1^2 u} \right)^{1/3} \exp \left[\left(\frac{q_1^2 u}{4} \right)^{1/3} \frac{3i + 3\sqrt{3}}{2} \right], \quad (59)$$

$$\left(\frac{q_1^2 u}{4} \right)^{1/3} \gg 1, \quad \left(\frac{2u}{q_1} \right)^{2/3} \gg 1.$$

The condition $w_0 \gg 1$ provides large values of the oscillation phases in Eqs.(53) and (54) which is required by the WKB approximation. In these calculations we also used the condition $u \gg w$. It holds at the saddle point provided that $(u/w_0) = (2u/q_1)^{2/3} \gg 1$, or $u \gg q_1/2$. The last condition determines the lower border of the asymptote in Eq.(59), in the regions where $q_1 > 2$.

According to Eq.(59), in the asymptotic region the amplitude of the bunch centroid $|Z(x, u)|$ increases in the time proportional to $\exp \left[(t/\tau)^{1/3} \right]$, where

$$\frac{1}{\tau} = \omega_0 (\Delta\nu_\beta)_{\max} \frac{N_b r_0 \lambda_b(0) \sigma_s^2}{2\sigma_y(\sigma_x + \sigma_y)} \left(\int_x^\infty \sqrt{g(x_1)} dx_1 \right)^2, \quad (60)$$

$(\Delta\nu_\beta)_{\max}$ is calculated using Eq.(24) and ω_0 is the revolution frequency of positrons in the ring. The fact that the instability growthrate depends on the position in the bunch is one of the specific features of the beam breakup instabilities (see, e.g. in Ref.[9]). The asymptotic behavior of $Z(x, u)$ described in Eq.(59) qualitatively agrees with that calculated for the beam breakup instability due to the interaction of the bunch with a sequence of resonant cavities (see, e.g. in Ref.[11]). This coincidence occurs due to similar linear initial increase in the wakefields responsible for the electron cloud instability (see in Eq.(16)) and for the instability calculated in Ref.[11]. On the other hand, this asymptote disagrees with results of calculations of the asymptotic growth of the amplitudes of the bunch centroid due to the electron cloud instability reported in Ref.[5] and predicted the growth $|Z(x, t)| \propto \exp \left(\sqrt{t/\tau} \right)$. The last asymptote is rather specific for a sudden switching on of the bunch wakefields. We remind the reader that simple asymptotic expression in Eq.(59) was calculated using a simplified initial distribution of the bunch centroid along the bunch. For more general initial conditions the asymptotic growth of the bunch centroid should be calculated substituting $y_{1,2}(p, x)$ from Eqs.(53) and (54) in Eq.(41) directly.

5 The solvable model

Apart from other cases, Eq.(9) can be solved analytically, if we assume that the linear density of the bunch is given by the exponential function:

$$\lambda_b(z) = \frac{1}{2\sigma_s} \exp \left(-\frac{|z|}{\sigma_s} \right). \quad (61)$$

This function has smooth tails and decays quickly enough when $|x| \rightarrow \infty$. Substituting this expression in Eq.(2), we rewrite Eq.(9) in the following form:

$$y_{1,2}'' + q^2 e^{-|x|} y_{1,2} = 0. \quad (62)$$

Using

$$W = y_1(x) \frac{dy_2(x)}{dx} - \frac{dy_1(x)}{dx} y_2(x) = -\frac{1}{\pi},$$

we find that Eq.(62) has the following linearly independent solutions:

$$y_1(q, x) = \begin{cases} J_0(2qe^{-\frac{x}{2}}), & x > 0, \\ aJ_0(2qe^{\frac{x}{2}}) + bN_0(2qe^{\frac{x}{2}}), & x < 0, \end{cases} \quad (63)$$

$$y_2(q, x) = \begin{cases} N_0(2qe^{-\frac{x}{2}}), & x > 0, \\ cJ_0(2qe^{\frac{x}{2}}) - aN_0(2qe^{\frac{x}{2}}), & x < 0. \end{cases} \quad (64)$$

Here, $J_0(x)$ and $N_0(x)$ are the Bessel and Neumann functions of the zero order (see, e.g. in Ref.[12]) and

$$a = -\pi q (J_0(2q) N_1(2q) + J_1(2q) N_0(2q)), \quad (65)$$

$$b = 2\pi q J_1(2q) J_0(2q), \quad c = -2\pi q N_1(2q) N_0(2q).$$

Substituting these functions in Eq.(15), we can calculate the kernel $K(x, x_1)$ and other relevant functions defined in the previous Sections². For example, let us calculate the function $X(x, u)$ neglecting the cloud pinching. For simplicity, we assume that initially the bunch centroid is constant along the bunch $X(x, 0) = 1$. Then, according to Eq.(45) the amplitude $X(x, \omega)$ reads

$$X(x, \omega) = \frac{i}{\omega + 1} + \frac{iy_1(p, x)}{\omega(\omega + 1)}, \quad p^2 = q^2 \frac{\omega + 1}{\omega}, \quad (66)$$

while

$$Z(x, u) = 1 + \int_{-\infty}^{\infty} \frac{d\omega}{2\pi i} \frac{1 - y_1(p, x)}{\omega(\omega + 1)} e^{-i\omega u}, \quad \text{Im}\omega > 0 \quad (67)$$

²One more solvable example present the case, where the linear density of the bunch reads

$$\lambda(z) = \frac{1}{2\sigma \cosh^2(z/\sigma)}, \quad g(x) = \frac{1}{\cosh^2(x)}.$$

and where $y_1(q, x) = P_\mu(\tanh(x))$, $y_2(q, x) = Q_\mu(\tanh(x))$, $\mu = [\sqrt{4q^2 + 1} - 1]/2$, while $P_\mu(z)$ and $Q_\mu(z)$ are the Legendre functions of the first and of the second kind, $W = 1$.

The value of the integral in the right-hand side of this expression is determined by the residue of the integrand at the essential singularity point $\omega = 0$.

Simple expressions for $Z(x, u)$ can be obtained in the region $x > 0$ (the head-on part of the bunch). Substituting in Eq.(67) the first line of Eq.(63) and using

$$1 - y_1(p, x) = \sum_{m=1}^{\infty} \frac{(-qe^{-x})^m (1 + \omega)^m}{(m!)^2 \omega^m},$$

we obtain

$$Z(x, u) = 1 + \sum_{m=1}^{\infty} \frac{(-q^2 e^{-x})^m}{(m!)^2} [L_m(iu) - L_{m-1}(iu)]. \quad (68)$$

Here,

$$L_m(x) = \frac{1}{m!} e^x \frac{d^m}{dx^m} [x^m e^{-x}] = m! \sum_{k=0}^m \frac{(-x)^k}{(k!)^2 (m-k)!} \quad (69)$$

are Laguerre polynomials (see in Ref.[12]). Since

$$\frac{L_m(iu) - L_{m-1}(iu)}{m!} = \sum_{k=1}^m \frac{(-iu)^k}{(k!)^2 (m-k)!} \frac{k}{m},$$

we can also rewrite Eq.(68) in the following form:

$$Z(x, u) = 1 + \sum_{m=1}^{\infty} Z_m(x, u), \quad (70)$$

where

$$Z_m(x, u) = \frac{(-q^2 e^{-x})^m}{m!} \sum_{k=1}^m \frac{(-iu)^k}{(k!)^2 (m-k)!} \frac{k}{m}. \quad (71)$$

The relative importance of subsequent terms in the series in Eq.(70) can be estimated using the picture in Fig. 1. This graph shows that the series in Eq.(70) converges well even for very large values of u .

Although the series in the right-hand side of Eq.(68) converges well, this expression is not very convenient for fast analytic calculations of $X(x, u)$ in the asymptotic region $u \gg 1$. To evaluate this asymptote we rewrite Eq.(67) like follows:

$$Z(x, u) = 1 + u \int_{-\infty}^{\infty} \frac{dw}{2\pi i} \frac{1 - J_0\left(qe^{-x/2} \sqrt{1 + (u/w)}\right)}{w(w+u)} e^{-iw}, \quad \text{Im}w > 0, \quad (72)$$

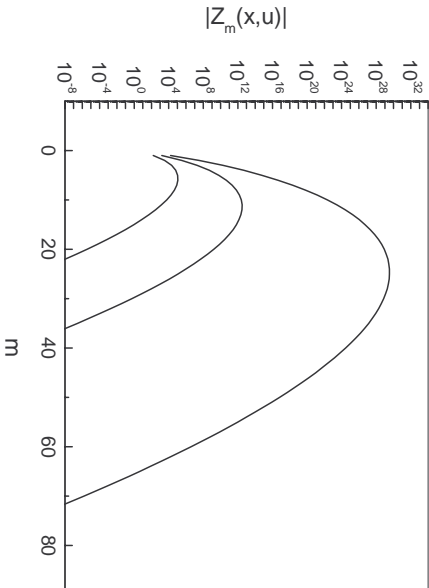


Figure 1: Dependence of $|Z_m(x; u)|$ on the row number m ; $x = 0$, $q = 4$, from top to bottom $u = 1000, 100, 10$.

and repeat the calculations described at the end of the previous Section. Assuming that the integration contour lies in the region where $u \gg |w|$ and $q^2 e^{-x} u \gg |w|$, using the asymptotic expressions for the Bessel function, we obtain ($w_0 = [q^2 e^{-x} u]^{1/3}$)

$$Z(x, u) \simeq \frac{i}{\pi \sqrt{6} w_0} \exp \left[-\frac{3}{2} w_0 + \frac{3\sqrt{3}}{2} w_0 \right], \quad w_0 \gg 1, \quad u \gg w_0. \quad (73)$$

In our solvable model the function q_1 from Eq.(55) reads $q_1 = 2q e^{-x/2}$ ($x > 0$). Comparing Eqs.(73) and (59), we find that the asymptote in Eq.(73) differs from that in Eq.(59) only by the factor of $\sqrt{2}$ and, therefore, both asymptotes almost coincide. So that these solutions do not indicate strong dependencies on initial distributions $X(x, 0)$ along the bunch ³.

As is seen in Fig. 2, Eq.(73) and Eq.(70) predict similar behavior of $|Z(x, u)|$ in the asymptotic region $w = (q^2 e^{-x} u)^{1/3} \gg 1$ with gradual decreases in the deviations between the data obtained using Eq.(70) and Eq.(73). However, for the data depicted in Fig. 2 the relative error in the calculation of $|Z(x, u)|$ using Eqs.(70) and (73) varies from about 40% for lower end in w to about 20% for the upper end of this graph in w . So that

³In fact, the difference between these two asymptotes growth with an increase in u approximately proportional to $(w_0/u)Z(x, u)$ which is substantially smaller than the values of $|Z(x, u)|$ in this region, but also is exponentially large in the absolute value.

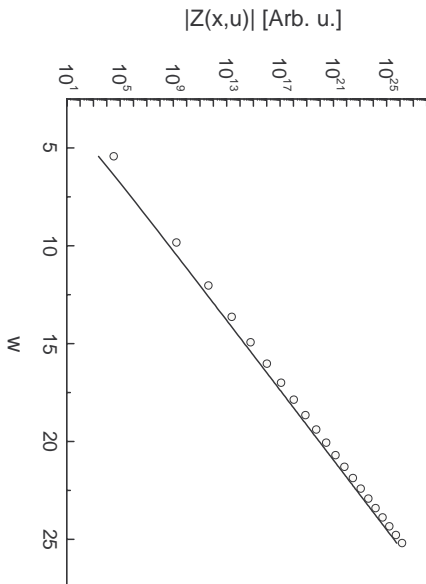


Figure 2: Dependence of $|Z(x, u)|$ on time (u); $x = 0$, $q = 4$, solid line: calculated using Eq.(68), open circles: asymptotic formula Eq.(73).

the accuracy of the asymptotic calculations is not very high. The range of the variations of the value w in this graph corresponds to the region $10 \leq u \leq 1000$. We also note that numerical values of $|Z(x, u)|$ depicted in Fig. 2 are very large and still will remain large even with reasonable decrease in the values of $Z(x, 0)$. That may break the initial assumption concerning linear dependencies of the forces acting on the cloud and bunch centroids and hence, can make predictions of such calculations less reliable.

The calculation of the integral in Eq.(67) in the region $x < 0$ results in a more complicated expression:

$$\begin{aligned}
 Z(x, u) = & 1 + 3iuxq^2 + \sum_{r=1}^{\infty} \frac{(-q^2 e^x)^{r+1}}{((r+1)!)^2} [L_{r+1}(iu) - L_r(iu)] \\
 & + \sum_{r=1}^{\infty} (-q^2)^r [L_{r+1}(iu) - L_r(iu)] \{2xq^2 H_r(x) + 4q^2 U_r(x)\}, \quad x < 0.
 \end{aligned} \tag{74}$$

Here,

$$H_r(x) = \sum_{m=0}^r \frac{F(-m, -m-1, 1, e^x)}{m!(m+1)!(r-m)!}, \tag{75}$$

$$U_r(x) = \sum_{m=0}^{r-1} \frac{F(-m, -m-1, 1, e^x) - e^{(r-m)x} \frac{(2m+1)!}{m!(m+1)!} h_{r-m}}{m!(m+1)!(r-m)!}, \tag{76}$$

$F(a, b, c, x)$ is the hypergeometric function and $h_k = \sum_{l=1}^k 1/l$, $k = 1, 2, \dots$. As could be expected in advance, the value $|Z(x, u)|$ increase proportional to $|x|$, when $x \rightarrow -\infty$.

6 Effects of the cloud pinching

Effects of the cloud pinching on the beam breakup instability of the bunch interacting with the electron cloud was studied solving Eq.(27) numerically. The kernel $K(x, x_1)$ in this equation was calculated using the described in the previous Section model with the exponential linear density of the bunch. In this case, Eq.(27) reads

$$\frac{dX(x, u)}{du} = -ir(x)X(x, u) - ir(x) \int_x^\infty dx_1 e^{-|x_1|} K(x, x_1) X(x_1, u) \quad (77)$$

The integral in the right-hand side of Eq.(77) was calculated using the trapezoidal rule. For that purpose, in the region $-5 \leq x \leq 5$ the bunch was divided on 500 slices and the integral was replaced by relevant finite sum. Correspondingly, Eq.(77) was replaced by the system of the differential equations:

$$\begin{aligned} \frac{dX_n}{du} = & -ir(x_n)X_n(u) \\ & -ir(x_n)h \left(\sum_{m=2}^{n-1} e^{-|x_m|} K(x_n, x_m) X_m + \frac{1}{2} e^{-|x_1|} K(x_n, x_1) X_1 \right). \end{aligned} \quad (78)$$

Here, $X_n(u) = X(x_n, u)$ are the slices centroids, the matrix $K(x_n, x_m)$ was calculated substituting in Eq.(15) the functions $y_{1,2}(q, x_n)$ from Eqs.(63) and (64), $h = 1/50$.

The factors $r(x_n)$ in the right-hand side of Eq.(78) were calculated using a simplified tracking program. In this program we traced the transverse motions of 500000 electrons placed in the central plane of the cylinder of the height h due to the space charge forces of the bunch with the linear density given in Eq.(61) and having a Gaussian round cross section. The rms radius of the bunch was taken as $\sigma_b^2 = \sigma_x \sigma_y$. For the calculations in the smoothed focusing approximation we used $\sigma_x = 600$ mkm and $\sigma_y = 60$ mkm which is close to the bunch parameters in KEKB. Typically, the number of particles in the bunch was taken as 7×10^{10} , the bunch length was taken as $\sigma_s = 7$ mm. These parameters correspond to $q = 4.365$. Initially the electrons

were uniformly distributed within the disk with the radius of $50\sigma_b \simeq 1$ cm. Initial kinetic energies of electrons (E_e) were uniformly distributed within the range $5 \text{ eV} \leq E_e \leq 200 \text{ eV}$ which qualitatively agrees with results of measurements reported in Ref.[4]. The program calculated the ratio of the density of the cloud on the closed orbit $n(x)$ to the unperturbed density of the cloud n_0 accounting the electrons within the radius of $0.3\sigma_b$ near the closed orbit of the bunch. The result of such calculations is shown in Fig. 3. The factors $r(x_n)$ were calculated normalizing the data depicted in Fig. 3 to one.

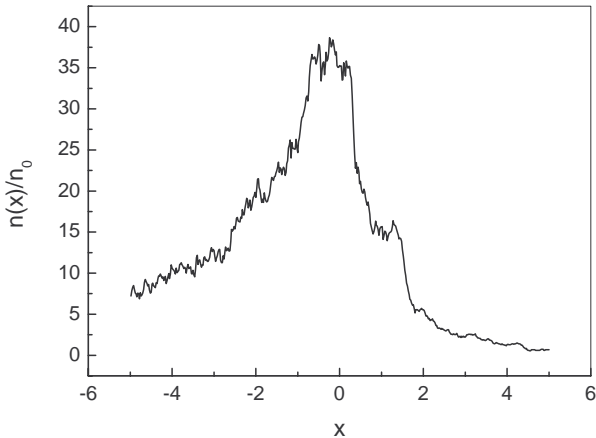


Figure 3: Dependence of the central density of the cloud $n(x)/n_0$ on the longitudinal distance in the bunch.

Equations in (78) were solved using the Runge-Kutta fifth-order and sixth-order method. The relative accuracy in these calculations was set as 0.01 %. In the most of calculations below we assumed that the initial cloud density is defined using the charge compensation condition $n_0 = N/(\pi\sigma_b^2 L_b)$, where L_b is the bunch spacing in the beam. For simplicity, in all numerical calculations below we took as initial condition the values $Z(x,0) = 1$ ($Z(x,u) = e^{iu} X(x,u)$). Since numerical results below are obtained solving the linear differential equations the results for all other (equal along the bunch) initial values of Z can be obtained scaling the reported data by a relevant factor. For this reason, in the figure captions below we mark units for Z as arbitrary units. Test calculations which were run neglecting the cloud pinching ($r(x) = 1$) resulted in the asymptotes $|Z(x,u)| \propto \exp([u/u_\tau]^{1/3})$

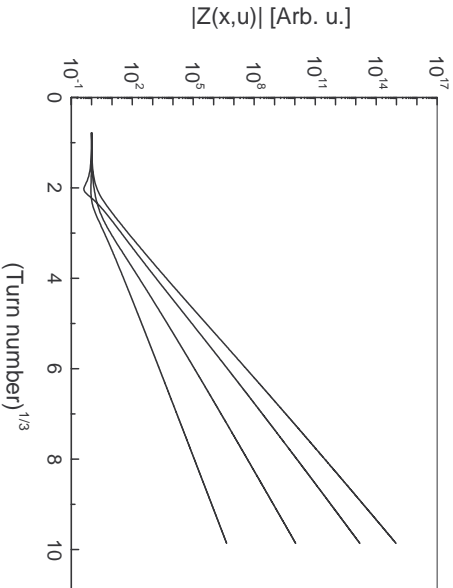


Figure 4: Dependence of the amplitudes of the bunch centroid on time (on the turn number). No cloud pinching, from top to bottom $|Z(x, u)|$ with $x = -2, -1, 0, 1$.

(Fig. 4) which agrees with results of the analytic calculations described in two previous Sections.

The cloud pinching results in the BNS damping of coherent oscillations of the bunch. For the electron cloud instability this damping manifests itself in substantial decreases in the amplitudes of the bunch centroids at large times (Fig. 5). The depth of the cloud pinching at a given point s on the closed orbit changes when the bunch passes the point s . It means that the cloud density near the closed orbit varies along the bunch. That results in proportional variations along the bunch of the betatron tunes of the particles which yield the BNS damping of coherent oscillations of the bunch. The non-monotonous dependence of the cloud density on x (Fig. 3) reduces the number of the resonant slices in the bunch and decreases the amplitudes of excited oscillations. Since the cloud pinching does not destroy the resonance conditions in the bunch completely, the BNS damping does not eliminate the electron cloud instability.

The oscillation amplitudes of the bunch interacting with the cloud without pinching begin to prevail that calculated accounting the cloud pinching after some time interval (Fig. 6). The point $x = -0.76$ in this Fig. is taken as an example and because the final amplitude of this slice is the maximum one (Fig. 5). For the case shown in Fig. 6, it occurs somewhere after

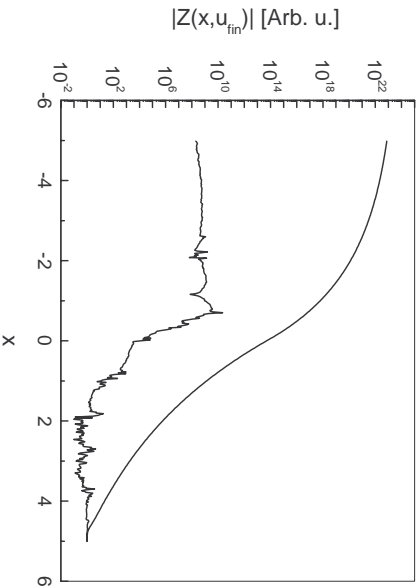


Figure 5: Dependence of the amplitudes of the bunch centroid on the longitudinal distance along the bunch x after 2000 turns; upper curve – no pinching, lower curve – with the cloud pinching.

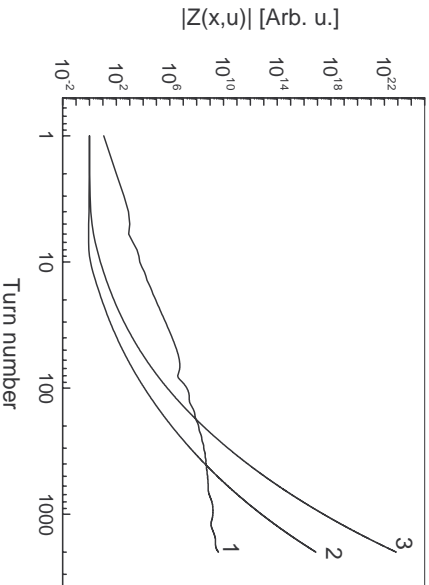


Figure 6: Dependence of the amplitudes of the bunch centroid on the time; curve (1) – $x = -0.76$, cloud pinching; curve (2) – $x = -0.76$, no cloud pinching; curve (3) – $x = -5$, no cloud pinching.

100 turns. During preceding time intervals the oscillation amplitudes of the bunch calculated taking into account the cloud pinching can be larger than that calculated neglecting the cloud pinching. Such a behavior could be expected beforehand. In any case, initial interactions of the bunch slices

via the cloud excite the oscillations of the subsequent slices by the preceding ones. The BNS damping begins to suppress the oscillations only after the time interval corresponding to the betatron frequency deviation in the bunch. On the other hand, the cloud pinching together with the BNS damping increases the strength of the excitation of the oscillations of the coupled slices resulting in larger initially excited amplitudes.

In both cases and in agreement with general theory of the beam breakup instability, the amplitudes of oscillations in the tail-on regions of the bunch substantially exceed that in the head-on parts of the bunch. However, in the case of the calculations ignoring the cloud pinching such an increase is described by smooth monotonous functions of x . On the contrary, the cloud pinching results in the appearance in the dependence of $|Z(x, u)|$ on x of sharp peaks.

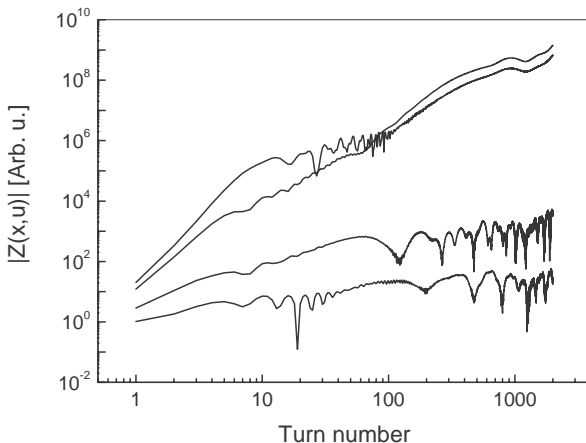


Figure 7: Dependence of the amplitudes of the bunch centroid on time (on the turn number). Cloud pinching, from top to bottom at 10 turns: $|Z(x, u)|$ with $x = -2, -1, 0, 1$.

The BNS damping due to the electron cloud pinching changes the character of the time dependence of the bunch centroid oscillation amplitudes (Fig. 7). Without the cloud pinching these dependencies are proportional to quasi-exponential functions (see, e.g. in Eq.(73)). As is seen in Fig. 7, due to the cloud pinching the oscillation amplitudes in the tail-on part of the bunch ($x \leq 0$) and at large times become proportional to the power functions of the time. For example, for the turn number exceeding 300 the oscillation

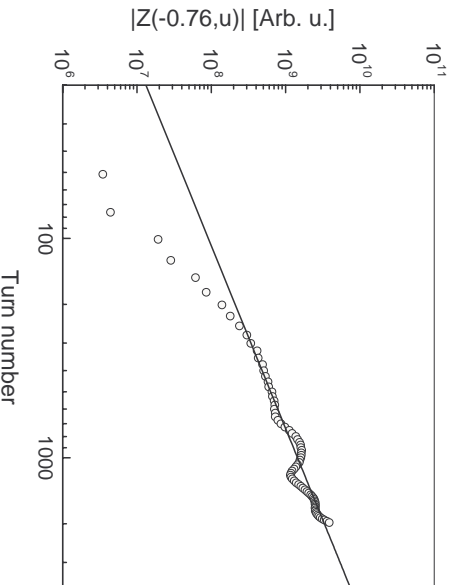


Figure 8: Dependence of the amplitude of the bunch centroid $|Z(x, u)|$ on time (on the turn number). Cloud pinching, $x = -0.76$, open circles – simulations, solid line – the fitting curve $|Z(-0.76, u)| \propto u^{1.2}$.

amplitude $|Z(-0.76, u)|$ is fitted well by the function $|Z(-0.76, u)| \propto u^{1.2}$ (Fig. 8). The reasons for such time dependencies can be explained inspecting Fig. 3. We again remind the reader that, generally, the beam breakup instability occurs due to the resonant excitations of the oscillations of subsequent slices of the bunch by the preceding ones. Without cloud pinching the tunes of the betatron oscillations of all slices in the bunch coincide so that the number of the resonant slices along the bunch is infinitely large. It results in the cumulative resonant oscillation excitation and in quasi-exponential growth of the amplitudes in time. On its turn and as we already mentioned, the cloud pinching modulates the betatron tunes along the bunch proportional to the ratio $n(x)/n_0$ (Fig. 3). As is seen in this graph, in the case of the cloud pinching only few slices along the bunch can have equal betatron tunes and hence, can excite their oscillations in the resonance. The finite number of the resonant slices results in an increase in the oscillation amplitude proportional to a power of the time. Although it is not shown, in the initial part of this graph the value of $|Z(-0.76, u)|$ varies proportional to u^4 . According to the approximations used in this paper, the growthrates of the discussed instabilities should not be too high. For the beam breakup instabilities we can define these values using

$$\delta = R_0 \frac{d \ln |Z(x, u)|}{ds}. \quad (79)$$

Since the beam breakup instability has no eigenvalue solutions, the values $\delta(x, u)$ depend both on the position along the bunch and on the time (u). We calculated the growthrates of the discussed instabilities using the data depicted in Figs. 7 and 4. As is seen in Fig. 9, the maximum value of the

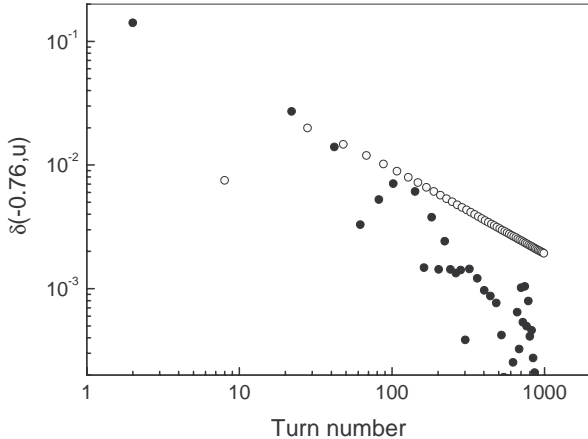


Figure 9: Dependence of the growthrate of the bunch centroid at $x = -0.76$ on time (on the turn number). Full circles - cloud pinching, open circles - no cloud pinching, only increments are shown.

growthrate $\delta(-0.76, u)$ is approximately four times lower than $(\Delta\nu_0)_{\max}$ for the bunch interacting with the pinched cloud

$$[\delta(-0.76, u)]_{\max} \simeq 0.140, \quad (\Delta\nu_0)_{\max} \simeq 0.544. \quad (80)$$

For the case without the cloud pinching, the value $[\delta(-0.76, u)]_{\max} = 0.031$ about two times exceeds $\Delta\nu_\beta \simeq 0.014$.

Inspecting the growths of the bunch oscillating amplitudes in time for different bunch intensities (Fig. 10), we find that for low bunch intensities (the lower curve in Fig. 10) the instability is depressed by the BNS damping. Without the cloud pinching the oscillation amplitude of this slice increases proportional to $\exp([u/u_\tau]^{1/3})$ and within the range shown in Fig. 10 reaches substantial values. As is seen in Fig. 10, the oscillations of high intensity bunches ($N \geq 3 \times 10^{10}$) grow systematically especially during initial period

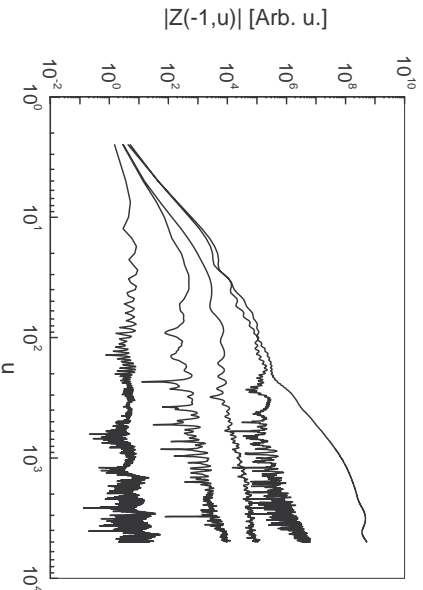


Figure 10: Dependence of $|Z(x, u)|$ at $x = -1$ (an example) on time u . Cloud pinching, from top to bottom: $N/10^{10} = 7, 6.5, 5, 3$ and 1 .

of the instability. Since the amplitudes increase proportional powers of the time, this fact can explain an existence of the threshold bunch current for the bunch transverse sizes blowups phenomenon. Particular value of this threshold depends on the oscillation damping mechanism.

In Fig. 10 we used u as an independent variable. With accepted here assumptions, the time dependencies of the oscillation amplitudes shown in this graph depend only on the bunch density and do not depend on the initial cloud density.

If ν_s is the tune of the synchrotron oscillations of the bunch particles, the beam breakup description of coherent oscillations of the bunch holds for the turn numbers which are substantially lower than $1/\nu_s$. For example, for KEKB $\nu_s = 0.025$, so that for this ring the beam breakup approximation may give reliable descriptions of coherent oscillations only during the first 10 turns. In the realistic case, when the cloud pinching is taken into account, the growthrates of the amplitudes of dipole oscillations exceed the value ν_s (Fig. 9). As is seen in Fig. 7, the growthrates in the central part of the bunch ($|x| \rightarrow 0$) and of the head-on parts of the bunch are lower than the mentioned numbers. The beam breakup description of coherent oscillations of these parts of the bunch demands substantially lower values of ν_s .

Another application of these calculation is the description of the coherent fluctuations with the average generation frequency exceeding the frequency of the synchrotron oscillations ω_0/ν_s . Such fluctuations (coherent oscillations

of the bunch and of the cloud with random amplitudes and phases) can be generated due to frequency spreads of the bunch and of the cloud. These spreads substantially exceed the frequency of the synchrotron oscillations of particles.

7 Conclusion

We have studied both analytically and numerically several aspects of the singlebunch dipole beam breakup instability of the positron bunch due to its interaction with electron clouds. The linear density of the bunch was assumed to be a smooth function of the longitudinal coordinate of the positron in the bunch. For particular calculations we used the linear density defined by the exponential function in Eq.(61). In this case, the fundamental solutions for the electron cloud oscillations $y_{1,2}(q, x)$ can be found analytically. That can simplify both analytical and numerical studies of the beam breakup oscillations of the positron bunch interacting with the electron cloud.

Without the cloud pinching the expressions describing the distribution of the bunch centroids along the bunch as well as their dependencies on time are calculated analytically using the set of the fundamental solutions $y_{1,2}(p, x)$, where $p = q\sqrt{(1+\omega)/\omega}$, $\text{Im}\omega > 0$. Although, generally, the oscillation amplitudes are described by complicated expressions those can be simplified in the asymptotic region in time ($[q_1^2 u/4]^{1/3} \gg 1$) where the amplitudes grow proportional to $\exp([t/\tau]^{1/3})$. This behavior qualitatively agrees with results of calculations obtained in Ref.[11] for the beam breakup instability of a bunch in linacs and disagrees with results of the calculations concerning the electron cloud instability reported in Ref.[5] where it was found that in the asymptotic region the amplitudes grow proportional to $\exp(\sqrt{t/\tau})$. The asymptotic behavior calculated in this paper and in Ref.[11] occur due to linear increase in the wakefields in the cloud at small distances $|x - x_1|$. This case occurs in the case of the electron cloud instability. On the contrary, the result of the paper [5] corresponds to a sudden switching-on of the wakefields. This discrepancy is a result of incorrect calculations with basic equations in Ref.[5].

One of the main objectives of this paper was the study of the influence of the electron cloud pinching and of the associated modulation of the tunes of betatron oscillations of positrons on the stability of coherent oscillations of the bunch. The calculations show that the cloud pinching substantially increases the tuneshifts of positrons due to the space charge fields of the cloud.

These tuneshifts are so big that the space charge fields of the cloud may result in the instability of incoherent oscillations of positrons and in corresponding increase in the transverse sizes of the bunch. For coherent oscillations of the bunch the electron cloud pinching results in the BNS damping of coherent oscillations of the bunch. However, the BNS damping affects the oscillation amplitudes after large time intervals. Initially, the pinching of the cloud makes the instability more rapid. Contrary to the case of ordinary BNS damping (see, e.g. in Ref.[8]), in the electron cloud instability the cloud pinching yields both the deviations of the betatron tunes along the bunch and the modulation (as well as an increase) along the bunch of coherent tune shifts of the slices. Moreover, the betatron tunes due to the cloud pinching are not a monotonous functions of x . Therefore, the tunes of some slices along the bunch can coincide. The interactions of such slices is resonant. For this reasons, the BNS damping due to the cloud pinching does not suppress the instability, but makes it substantially weaker at large time intervals. Besides, this damping changes the growth-law of the oscillation amplitudes from the quasi-exponential to the power function of the time.

More generally, the cloud pinching leads to the modulations of the betatron tunes of particles by their synchrotron oscillations. Beyond the beam breakup approximation and if the pinching is strong, that may result in additional couplings of the synchro-betatron modes of coherent oscillations of the bunch which may change the thresholds of the mode-coupling instabilities of the bunch.

I am indebted to N. Dikansky, H. Fukuma, S. Kurokawa, K. Ohmi and K. Oide for their valuable comments and discussions.

Appendix A

The limit to the rectangular bunch linear density

According to Eqs.(15) and (19) if the linear density of the bunch is a smooth function of z , then the wake function of the bunch due to its interactions with the electron cloud, generally, is not a function of $z' - z$. That occurs only in a special case, where the linear density of the bunch is a step function of z , so that

$$g(z) = \begin{cases} 1, & |z| \leq \sigma_s, \\ 0, & |z| > \sigma_s. \end{cases} \quad (\text{A.1})$$

Here, $2\sigma_s$ is the bunch length. For the bunch with such a linear density Eq.(9) is reduced to

$$\frac{d^2 y}{dz^2} + k_c^2 y = 0, \quad k_c = \frac{\omega_c}{v}, \quad (\text{A.2})$$

while the functions y_1 and y_2 read

$$y_1 = e^{ik_c z}, \quad y_2 = e^{-ik_c z}, \quad (\text{A.3})$$

with

$$W = y_1 \frac{dy_2}{dz} - \frac{dy_1}{dz} y_2 = -2ik_c. \quad (\text{A.4})$$

Substituting these functions in Eq.(15), we obtain the kernel which was previously calculated for this case in Ref.[6]:

$$\begin{aligned} K_0(z, z') &= \frac{k_c^2}{-2ik_c} [\exp(-ik_c [z' - z]) - \exp(ik_c [z' - z])] \\ &= k_c \sin(k_c [z' - z]). \end{aligned} \quad (\text{A.5})$$

Now, we expect that similar kernel can be obtained in some special region of the problem parameters substituting the functions $y_{1,2}(q, x)$ defined in Eqs.(63) and (64) in Eq.(15). Namely, we inspect the case, where $q \gg 1$ and $|z| \ll \sigma_s$, so that the arguments of the Bessel functions in Eqs.(63) and (64) reach the asymptotic region. For simplicity, we present the calculations for the region where $x > 0$ and $x' > 0$ (all other regions give similar results). In the region of the interest we write:

$$y_1(x) = J_0\left(2qe^{-x/2}\right), \quad y_2(x) = N_0\left(2qe^{-x/2}\right), \quad x = \frac{z}{\sigma_s}, \quad q = k_c \sigma_s, \quad (\text{A.6})$$

and [12]

$$J_0 \left(2qe^{-x/2} \right) \simeq \sqrt{\frac{1}{\pi q}} e^{x/4} \cos \left(2qe^{-x/2} - \frac{\pi}{4} \right), \quad (\text{A.7})$$

$$N_0 \left(2qe^{-x/2} \right) \simeq \sqrt{\frac{1}{\pi q}} e^{x/4} \sin \left(2qe^{-x/2} - \frac{\pi}{4} \right). \quad (\text{A.8})$$

Substituting these expressions in Eq.(15), we obtain

$$K_0(x, x') = -\pi q^2 e^{-x'} [y_2(x') y_1(x) - y_2(x) y_1(x')] \quad (\text{A.9})$$

$$= -qe^{-x'} \sqrt{\exp\left(\frac{x'+x}{2}\right)} \sin\left(2qe^{-x'/2} - 2qe^{-x/2}\right). \quad (\text{A.10})$$

In the region $x, x' \ll 1$ we replace

$$e^{-x/2} \simeq 1 - \frac{z}{2\sigma_s},$$

and

$$\exp\left(\frac{x+x'}{2}\right) \simeq 1, \quad e^{-x'} \simeq 1,$$

to find

$$K_0(x, x') \simeq q \sin(k_c [z' - z]), \quad (\text{A.11})$$

or using the variables z and z'

$$K_0(z, z') \simeq k_c \sin(k_c [z' - z]), \quad (\text{A.12})$$

which agree with Eq.(A.5). According to these calculations we conclude that for the bunches with smooth dependencies of the linear density on z the simple expression for the wake fields obtained in Ref.[6] (Eq.(A.5), or similar) can be used only for central slices ($|z| \ll \sigma_s$) in very long bunches ($k_c \sigma_s \gg 1$).

References

- [1] K. Ohmi and F. Zimmermann, *Phys. Rev. Lett.* **85**, 3821 (2000).
- [2] Y. Funakoshi, K. Akai, N. Akasaka, K. Bane, et al., in *Proceedings of EPAC 2000, Vienna, Austria*, p. 28 (2000).
- [3] J. Seeman, Y. Cai, J. Clendenin, F.-J. Decker, et al., *ibid*, p. 38.
- [4] H.Fukuma, *Electron Cloud Effects at KEKB*, In *Proceedings of ECLLOUD'02 Workshop*. CERN-2002-001.
- [5] T. F.Wang, P. J. Channell, R. J. Macek and R. C. Davidson, *Phys. Rev. ST Accel. Beams*, **6**, 014204 (2003).
- [6] K. Ohmi, F. Zimmermann and E. Perevedentsev, *KEK Preprint 2001-14*, May 2001.
- [7] D. V. Pestrikov, *Phys. Rev. ST Accel. Beams*, **7**, 119201 (2004).
- [8] V.E. Balakin, A.V. Novokhatski, V.P. Smirnov, In *Proceedings of the XII Intern. Conf. on High Energy Accel.*, p. 119, Fermilab 1983.
- [9] N.S. Dikansky, D.V. Pestrikov. *Physics of Intense Beams and Storage Rings*. AIP PRESS, New York, 1994.
- [10] J. Heading. *An Introduction to Phase-Integral Method*. John Willey, New York, 1962.
- [11] A. Chao, B. Richter, Ch. Yao. *Nucl. Instr. and Meth. in Phys. Res.* 178, p. 1 (1980).
- [12] I. S. Gradshteyn, I. M. Ryzhik, *Table of Integrals, Series, and Products*, Fifth Edition, Edited by Allan Jeffrey, Academic Press, 1994.

D.V. Pestrikov

**Dipole beam breakup electron cloud instability
of a relativistic positron bunch
with a smooth model linear density**

Д.В. Пестриков

**Дипольная неустойчивость
релятивистского позитронного пучка
с гладкой линейной плотностью,
взаимодействующего с электронными облаками**

Budker INP 2005-6

Ответственный за выпуск А.М. Кудрявцев
Работа поступила 18.02.2005 г.

Сдано в набор 20.02.2005 г.

Подписано в печать 22.02.2005 г.

Формат бумаги 60×90 1/16 Объем 2.2 печ.л., 1.8 уч.-изд.л.

Тираж 105 экз. Бесплатно. Заказ № 6

Обработано на IBM PC и отпечатано на
ротапринте ИЯФ им. Г.И. Будкера СО РАН

Новосибирск, 630090, пр. академика Лаврентьева, 11.